Journal of Biomolecular NMR, **26:** 283–295, 2003.
KLUWER/ESCOM

Assessing the effects of time and spatial averaging in ^{15}N chemical shift/^{15}N-^{1}H dipolar correlation solid state NMR experiments

Suzana K. Straus*,**, Walter R.P. Scott* & Anthony Watts
Department of Biochemistry, University of Oxford, South Parks Road, Oxford OX1 3QU, U.K.

Received 16 October 2002; Accepted 11 March 2003

Key words: mobility of membrane helices, mosaic spread, PISA wheels, PISEMA, time averaging

Abstract

The effect of time and spatial averaging on ^{15}N chemical shift/^{1}H-^{15}N dipolar correlation spectra, i.e., PISEMA spectra, of α-helical membrane peptides and proteins is investigated. Three types of motion are considered: (a) Librational motion of the peptide planes in the α-helix; (b) rotation of the helix about its long axis; and (c) wobble of the helix about a nominal tilt angle. A 2ns molecular dynamics simulation of helix D of bacteriorhodopsin is used to determine the effect of librational motion on the spectral parameters. For the time averaging, the rotation and wobble of this same helix are modelled by assuming either Gaussian motion about the respective angles or a uniform distribution of a given width. For the spatial averaging, regions of possible ^{15}N chemical shift/^{1}H-^{15}N dipolar splittings are computed for a distribution of rotations and/or tilt angles of the helix. The computed spectra show that under certain motional modes the ^{15}N chemical shift/^{1}H-^{15}N dipolar pairs for each of the residues do not form patterns which mimic helical wheel patterns. As a result, the unambiguous identification of helix tilt and helix rotation without any resonance assignments or on the basis of a single assignment may be difficult.

Abbreviations: r.m.s. – root mean square; CSA – chemical shift anisotropy; D – dipolar coupling; CS/D – ^{15}N chemical shift/^{15}N-^{1}H dipolar coupling; MD – molecular dynamics; d.o.f. degrees of freedom; PISA – polarisation index of the slant angle; PISEMA – polarisation inversion with spin exchange at the magic angle; c.o.m. – centre of mass.

Introduction

With the improved resolution now obtainable in solid state NMR, structural and dynamics studies of membrane embedded peptides and proteins (Opella et al., 1999; Marassi et al., 1999; Song et al., 2000; Glaubitz and Watts, 1998) are now emerging. In the case of oriented static samples, the improvement in resolution is achieved by means of two- or three-dimensional experiments, which typically correlate the ^{15}N chemical shift with the ^{1}H-^{15}N dipolar splitting and/or with the ^{1}H chemical shift (Ramamoorthy et al., 1996, 1999) and incorporate the efficient homonuclear ^{1}H decoupling method of frequency-switched Lee–Goldburg (Bielecki et al., 1989). For the PISEMA experiment (Ramamoorthy et al., 1999), the improvement in resolution over separated local field experiments (Waugh, 1976) makes the identification of individual resonances for each peptide plane in a ^{15}N chemical shift/^{15}N-^{1}H dipolar (CS/D) correlation map possible. Recent structures of membrane peptides solved using this approach include M2 (Opella et al., 1999; Song et al., 2000).

Recently, it has been proposed that the CS/D pairs obtained for the peptide planes of an α-helix (Marassi and Opella, 2000; Wang et al., 2000; Denny et al., 2001) and a β-sheet (Marassi, 2001) form characteristic patterns in the PISEMA spectra. These patterns are named PISA wheels, which for α-helices mimic the helical wheel patterns (Schiffer and Edmundson,

*Current address: Department of Chemistry, University of British Columbia, 2036 Main Mall, Vancouver, B.C., V6T 1Z1, Canada.
**To whom correspondence should be addressed. E-mail: sstraus@chem.ubc.ca

1967). The method has been proposed as a means by which the tilt angle between an α-helix and the plane of the lipid bilayer into which it is embedded can be determined, without the need for the assignment of spectral resonance peaks to individual helix residues. Moreover, it has been suggested that PISA wheels provide information on the rotation of the helix around its long axis (so called polarity) in the bilayer on the basis of a single assignment.

All theoretical discussions to date have considered the static case of an ideal helix ($\phi = -65°, \psi = -40°$), in which the peptide planes are inclined at the same angle with respect to the long axis of the helix. Furthermore, the fact that any configuration-dependent experimental observable, $\mathbf{A}^{\text{obs}}$, represents an average *over time*, denoted by $< \quad >$, and over *a number of molecules at any instant*, denoted by { }, has not yet been considered; i.e.,

$$\mathbf{A}^{\text{obs}} = \langle \{ \mathbf{A}(\mathbf{q}(t)) \} \rangle \,, \tag{1}$$

where $\mathbf{q}(t)$ denotes the time dependent coordinates of a molecule in the system. In Marassi and Opella (2000) and Wang et al. (2000), no motional averaging has been considered since it was assumed that nearly all residues in a polypeptide chain are immobile on time scales longer than milliseconds. It has also been assumed that there is no spatial orientational distribution (mosaic spread) of the polypeptides in the lipid matrix.

However, membrane peptides and proteins are dynamic (North and Cross, 1995; Huster et al., 2001) and can often adopt a range of orientations in lipids (Smith et al., 1994; Sizun and Bechinger, 2002). Although some of the few membrane protein systems studied to date by solid state NMR, namely bacteriorhodopsin (Bowers and Oldfield, 1988; Saito et al., 2000; Herzfeld et al., 1987), colicin E1 (Kumashiro et al., 1998), and the coat protein of the filamentous bacteriophage fd (Colnago et al., 1987; Cross and Opella, 1982), have been found to have essentially rigid backbones, many membrane proteins are dynamic in order to fulfil their biological functions (Qui et al., 1996; Prosser et al., 1991; Litman and Mitchell, 1996; Tieleman et al., 2001; Watts, 1998; Hubbell et al., 2000; Bowers and Oldfield, 1988; Bechinger, 2000). Librational motions of the peptide planes and variations of the helix rotation and helix tilt with respect to the membrane normal have been observed experimentally (North and Cross, 1995; Jones et al., 1998; Huster et al., 2001; Watts, 1998; Hubbell et al., 2000; Bowers and Oldfield, 1988) and predicted from molecular dynamics studies (Shen et al., 1997; Bachar and Becker, 2000; Woolf and Roux, 1994). For instance, r.m.s. (root mean square) librational amplitudes for all residues in gramicidin were found to be 5°–10° from solid state NMR (North and Cross, 1995) data and 15°–20° from molecular dynamics simulations (Woolf and Roux, 1994). The timescale of these librations was found to be on the order of pico- to nanoseconds. For the membrane-bound colicin Ia channel domain, even larger angular excursions (12–16°) in the backbone were found (Huster et al., 2001). Rotations about the long axis of a transmembrane helix also occur and are believed to be, in some cases, the mechanism by which ion channels open and close (Cordes et al., 2001; Johnson and Zagotta, 2001). This type of motion typically occurs on a time scale of milliseconds (Johnson and Zagotta, 2001), but has in some cases also been observed to be on the order of microseconds (Prosser and Davis, 1994). Not surprisingly, multiple identifiable conformations rather than continuous rotation have also been found to exist in transmembrane domains, e.g., there are four orientations of the EFG transmembrane domain (Jones et al., 1998). Finally, examples of spread in the tilt of the helix with respect to the membrane normal include experimental results obtained for melittin (Smith et al., 1994) and other model peptides (Sizun and Bechinger, 2002; Bechinger and Sizun, 2002), as well as simulations on polyalanine (Shen et al., 1997). The presence of spatial orientational distributions is expected to be prevalent below the lipid transition temperature T_c (Marsh, 1990), where the dynamics of membrane peptides and proteins are reduced and often result in a spread of molecular orientations or conformations.

Here, the effects of time and spatial averages on the CS/D pairs are considered by computer simulation for an experimentally determined helix structure. Three types of motion are considered, first individually and then in combination: (i) Librational motion of the peptide planes; (ii) rotation of the helix about its long axis; and (iii) wobble of the helix about a nominal tilt axis, relative to the static magnetic field. From these considerations, it can be assessed to what extent averaging effects inherent in the resultant solid state NMR experiments affect the spectra observed. The effect of motion on the accuracy in determining configurational parameters, such as the helix tilt angle and helix rotation, is discussed in light of these results.

Methods

The coordinates of an experimentally determined α-helix were used as a starting point for the investigations. The α-helix consists of residues 100–130 of bacteriorhodopsin (helix D), taken from the X-ray structure by (Sass et al., 2000) (PDB entry 1CWQ; resolution = 2.25 Å). This helix was chosen because it is the longest helix in the structure and is neither kinked nor significantly distorted. The long axis $\mathbf{h}^{\text{org}}$ of the helix, defined by the vector (5.144, −0.040, −36.257), was determined by modelling using the InsightII program (MSI) and verified by determining the centre of mass of the backbone atoms in the fragment. It is estimated that the error associated with the determination of $\mathbf{h}^{\text{org}}$ is on the order of ±2°.

A program was written in C to calculate the ^{15}N chemical shift and ^{15}N-^{1}H dipolar coupling for each peptide plane in the helix. The program allows the atoms of a helix to be rotated such that its long axis is parallel to an arbitrary vector $\mathbf{h}(\xi)$, where ξ is the angle between the direction of the magnetic field $\mathbf{B}_0 = (0, 0, 1)^T$ and the vector $\mathbf{h}(\xi)$. As the experimental parameters are invariant with respect to a rotation of the peptide plane around $\mathbf{B}_0$, we choose $\mathbf{h}(\xi) = (0.0, \sin(\xi), \cos(\xi))^T$. Furthermore, the program allows for the subsequent rotation of atom coordinates around the new helix axis $\mathbf{h}(\xi)$ by an angle ω.

The observables are determined by the atoms defining the normal vectors of the peptide planes $\mathbf{n}_i$, $i = 2, \ldots, N_{\text{seq}}$ (see supplemental material), where

$$\mathbf{n}_i = \mathbf{NH}_i \times \mathbf{CC}_i^{\alpha}, \tag{2}$$

N_{seq} denotes the number of residues in the helix, $\mathbf{NH}_i = \mathbf{H}_i - \mathbf{N}_i$, $\mathbf{CC}_i^{\alpha} = \mathbf{C}_i^{\alpha} - \mathbf{C}_{i-1}^{\alpha}$ and $\mathbf{X}_y$ denotes the coordinates of the X-atom in residue y. The angle α_i, measured between $\mathbf{NP}_i$ and $\mathbf{NH}_i$ in the peptide plane, is determined from

$$\alpha_i = \arccos\left(\frac{\mathbf{NP}_i \cdot \mathbf{NH}_i}{|\mathbf{NP}_i|\,|\mathbf{NH}_i|}\right), \tag{3}$$

where

$$\mathbf{NP}_i \;=\; \mathbf{P}_i - \mathbf{N}_i = \mathbf{B}_0 - \frac{\mathbf{B}_0 \cdot \mathbf{n}_i}{\mathbf{n}_i \cdot \mathbf{n}_i}\mathbf{n}_i, \tag{4}$$

and $\mathbf{P}_i$ is the projection of $\mathbf{N}_i + \mathbf{B}_0$ onto the peptide plane by its normal vector n_i. The angle β_i between $\mathbf{n}_i$ and $\mathbf{B}_0$ is calculated in a similar fashion to α_i. Finally, the chemical shift ^{15}N CS_i (in units of ppm) and the dipolar coupling ^{15}N-^{1}H D_i (in units of Hertz) can be determined from α_i and β_i:

$$^{15}\text{NCS}_i = \sigma_{11}\sin^2(\alpha_i - \theta)\sin^2(\beta_i) + \sigma_{22}\cos^2(\beta_i) + \sigma_{33}\cos^2(\alpha_i - \theta)\sin^2(\beta_i), \tag{5a}$$

$$^{15}\text{N} - {}^{1}\text{HD}_i = \frac{b_{\text{NH}}}{r_{\text{NH}}^3}\left[3\cos^2(\alpha_i)\sin^2(\beta_i) - 1\right], \tag{5b}$$

where σ_{11}, σ_{22} and σ_{33}, in units of ppm, and the angle θ are experimentally determined chemical shift anisotropy parameters, $b_{\text{NH}} = 12171.5$ Hz Å^3 is the NH dipolar coupling constant and r_{NH} is the experimentally determined length of the NH bond in Å.

The values used here for these parameters in the calculation of the ^{15}N CS for non-glycine residues were obtained by averaging all currently available CSA parameters in the literature (see supplemental material), for which the σ_{11} component lies in the peptide plane. The parameters for the glycine residues, which have markedly different values, were considered separately (see supplemental material). The average values used were: $\sigma_{11} = 56.3$ ppm, $\sigma_{22} = 79.0$ ppm, $\sigma_{33} = 224.0$ ppm and $\theta = 16.7°$ for all amino acids except glycines. For glycine residues, $\sigma_{11} = 45.6$ ppm, $\sigma_{22} = 66.3$ ppm, $\sigma_{33} = 211.6$ ppm and $\theta = 21.6°$. The chemical shifts are all relative to liquid NH_3 at room temperature.

For the calculation of the dipolar splitting ^{15}N-^{1}H D, an average NH bond distance of $r_{\text{NH}} = 1.066$ Å was used, as obtained from literature values (see supplemental material). Note that all NH bond lengths used to calculate the average were measured by solid state NMR methods, which are known to overestimate the bond length because librational motion as well as intramolecular vibrations reduce the measured dipolar interaction (Ishii et al., 1997).

An instantaneous CS/D pair $\nu_i(t) = (^{15}\text{NCS}_i(t), {}^{15}\text{N-}{}^{1}\text{H D}_i(t))$ for a given peptide plane i is dependent on the following configurational variables:

- the tilt of the helix with respect to $\mathbf{B}_0$, defined by angle $\xi(t)$,
- the angle of rotation about the helix axis, defined by $\omega(t)$,
- the angle between the helix axis and the ith peptide plane $\pi_i(t)$.

Thus, now considering averaging effects, the observed NMR spectrum for peptide plane i in the helix will be determined by

$$\nu_i^{\text{obs}} = \langle\{\nu_i(\xi(t), \omega(t), \pi_i(t))\}\rangle, \tag{6}$$

where $\langle\ \rangle$ and $\{\ \}$ denote a time average and an average over all molecules, respectively. The following condi-

tions must be met for the time and spatial averages to be equivalent:

- ergodicity: the assumption that time average is equal to the ensemble average.
  Here, we always assume this condition is fulfilled.
- infinite dilution: the assumption that the interactions between individual molecules are negligible, so that the motion of any given molecule is uncorrelated with the motion of any others in the system.
  Here, we assume that the condition of infinite dilution is fulfilled.
- molecular interconversion rates must be rapid compared to the time resolution of the NMR experiment. If this is not the case, a distribution of individual spectral intensities will be observed, rather than a single intermediate peak (chemical exchange (Ernst et al., 1987)).

Because of its rapid nature, we consider it safe always to treat the librational motion as a time average. The two slower motions are considered both as time averages and as spatial distributions. In the latter case, the individually calculated intensities are assigned equal weights in our model of motion, as there is no energetic difference between the conformations generated by a geometric transformation.

In order to calculate Equation 6 from computer simulation data, the correct distribution of the configurational parameters $\xi(t)$, $\omega(t)$, and $\pi_i(t)$ are needed. Because of the averaging assumptions, a simulation of a single molecule can be employed. The length of the simulation should be adequate for all relevant degrees of freedom to be well sampled. With respect to the degrees of freedom of interest here, only the rapid librational motions of the peptide planes, characterised by $\pi_i(t)$, are adequately sampled during the course of the 2 ns simulation. Equation 6 can nevertheless be evaluated by assuming certain probability distributions of $\xi(t)$ and $\omega(t)$ around given values of ξ_0 and ω_0 of interest. For time averages (fast motion) we calculate a weighted average:

$$\nu_i^{\mathrm{obs}}(\xi_0, \delta_\xi, \omega_0, \delta_\omega) = \sum_{k=1}^{N_{cfg}} \sum_{l=1}^{N_\xi} \sum_{m=1}^{N_\omega} \frac{1}{N_{cfg}} f_l^\xi f_m^\omega \nu(\xi_l, \omega_m, \pi_k^i), \quad (7)$$

where the N_{cfg} values for π_k^i are taken from a computer simulation. For the other degrees of freedom, we choose $n = 1 \ldots N_\gamma$ points around a value γ_0 from a distribution of width $2\delta_\gamma$ from either a uniform distribution ($\gamma_n = \gamma_0 - \delta_\gamma + 2\delta_\gamma(n-1)/N_\gamma$ and weight $f_n^\gamma = 1/N_\gamma$), or a Gaussian distribution ($\gamma_n = \gamma_0 + Z_n\sigma$ and $f_n^\gamma = \exp(-Z_n^2)$, where $Z_n = -\delta_\gamma + 2(n-1)\delta_\gamma/(N_\gamma - 1)$), for $\gamma = \xi$, $n = l$ and $\gamma = \omega$, $n = m$. Motion in a particular degree of freedom can be omitted by setting $N_\gamma = f_\gamma = 1$. In the case of $N_{cfg} = 1$, the coordinates of the crystal structure are used. Spectra of spatial distributions (slow motion) are simulated by plotting multiple points obtained from Equation 7 for discrete values of ξ and ω. The eleven combinations of these three degrees of freedom treated here are summarised in Table 1.

Molecular dynamics computer simulations of the helix fragment solvated in methanol were performed using the GROMOS96 (Scott et al., 1999; van Gunsteren et al., 1996) simulation package and the GROMOS96 43A1 force field (van Gunsteren et al., 1996). The technical details can be found in the supplemental material. Equation 7 was evaluated for residues 106–126 of the bacteriorhodopsin helix which remained α-helical throughout, as shown in Ramachandran plots (see supplemental material). The r.m.s. deviations of the peptide plane angles π_i for these residues were 10°–14° (data not shown).

Results

Static helix

In Figure 1, the calculated spectra obtained for the crystal structure of helix D in bR (residues 106–126) are presented. The CS/D pairs were calculated for ξ = 0°–90°, in steps of 18°. The value of ω was fixed at 0°. The spectra are plotted for dipolar transitions ranging within 11 kHz to −6 kHz, as in the convention adopted in, e.g., Wang et al. (2000). As ξ is varied from 0° (Figure 1a) to 90° (Figure 1e), the chemical shifts are displaced toward smaller ppm values. For the dipolar splitting, the value of ^{15}N-^{1}H D is largest and positive for $\xi = 0$, decreases with increasing ξ, is zero around the magic angle, and negative for ξ values larger than 54°. These shifts in the resonances agree with results previously reported in the literature (Marassi, 2001; Marassi and Opella, 2000; Wang et al., 2000).

Contrary to the calculated spectra for an ideal helix presented by Marassi and Opella (2000) and Wang et al. (2000), the CS/D pairs for consecutive residues do not form perfectly spherical helical wheels. This is due to the non-ideality of the experimentally determined structure of the D helix of bacteriorhodopsin considered here, as well as the use of separate CSA

Table 1. The combinations of averaging effects studied in this paper, where ξ denotes the angle between the magnetic field and the helix axis (tilt), ω denotes an angle of rotation of the helix around its own axis, and π denotes the angle between a peptide plane and the helix axis. When fast motion is assumed, a time average, denoted by $< >$, is taken over the respective d.o.f. When slow motion is assumed, a spatial distribution, denoted by { }, is calculated.

Case number	Variable parameters	Comment
1	$\nu_i(\xi_k, \omega_0, \pi_{i_0})$	Static helix: no motion
2	$\nu_i(\xi_k, \omega_0, \langle\pi_i(t)\rangle)$	Fast planar motion only
3	$\nu_i(\xi_k, \langle\omega(t)\rangle, \pi_{i_0})$	Fast axial rotation only
4	$\nu_i(\langle\xi(t)\rangle, \omega_0, \pi_{i_0})$	Fast tilt motion of helix only
5	$\nu_i(\xi_k, \langle\omega(t)\rangle, \langle\pi_i(t)\rangle)$	Fast axial and planar motions
6	$\nu_i(\langle\xi(t)\rangle, \omega_0, \langle\pi_i(t)\rangle)$	Fast tilt and planar motions
7	$\nu_i(\langle\xi(t)\rangle, \langle\omega(t)\rangle, \pi_{i_0})$	Fast tilt and axial motions
8	$\nu_i(\langle\xi(t)\rangle, \langle\omega(t)\rangle, \langle\pi_i(t)\rangle)$	All three fast motions
9	$\nu_i(\{\xi(t)\}, \omega_0, \langle\pi_i(t)\rangle)$	Fast planar motion with distribution of helix tilt
10	$\nu_i(\xi_k, \{\omega(t)\}, \langle\pi_i(t)\rangle)$	Fast planar motion with distribution of axial rotation
11	$\nu_i(\{\xi(t)\}, \{\omega(t)\}, \langle\pi_i(t)\rangle)$	Fast planar motion with distributions of tilt and axial rotation

parameters for the six glycines. For a given (α, β) pair, the ^{15}N CS of a glycine residue will appear at a lower field position than the ^{15}N CS for all other amino acids. As a result, the connectivities between consecutive residues are not as circular, but are rather jagged and smeared out.

As an indicator of helix tilt, the spectra are clearly distinctive for small values of ξ, where small changes in the tilt angle translate into large changes in the parameters, in particular for the dipolar splitting. These clear distinctions are more difficult as ξ approaches 80°–90°. Thus, if the resonances are not assigned, a comparison of the simulated and experimental spectra could yield information of helix tilt for ξ in the range of 0°–70° in principle.

Calculations where ω was allowed to vary by 90° were also performed to assess whether the simulated spectra can be used to determine helix polarity (Marassi and Opella, 2000; Wang et al., 2000) on the basis of a single assignment. As the calculated CS/D pairs for helix D do not form distinctive PISA wheels, the identification of different polarities is not as straightforward as in (Marassi and Opella, 2000), but the trends observed are similar. In other words, the CS/D pairs move in a circular fashion by approximately 90° in the simulated spectra for each change in $\omega = 90°$.

Case 2: Fast planar librational motion only

If Equation 7 is now evaluated considering planar librational motion, then the ^{15}N chemical shift/^{15}N-^{1}H dipolar pairs shift, as illustrated in Figure 2. Again, the CS/D pairs were calculated for $\xi = 0°$–90°, in steps of 18°, and ω was fixed at 0°. Librational motion was introduced by averaging over the coordinates generated using 200 configurations from the 2 ns molecular dynamics simulation.

Overall, the CS/D pairs cluster more than in the case of the static helix (Figure 1), causing the peaks to overlap, particularly for certain values of ξ (e.g., Figure 1d). As a result, the connectivities arising from consecutive residues do not form clear helical wheels. This is particularly true for ξ values greater than 50°.

Moreover, as in the static case, the chemical shift and dipolar splittings shift as a function of ξ, but the range in which small changes in ξ translate into large changes in the chemical shift and dipolar splittings is narrowed. Thus, the range of ξ for which the helix tilt can be determined unambiguously, without any assignments, is approximately limited to $\xi = 0°$–55°.

Case 3: Fast axial rotation only

In the case of fast axial rotation, two motional weighting schemes were considered. The first involved rotations of the helix around a fixed ω angle with a Gaussian distribution of width $\pm 20°$. This is used to simulate rapid Brownian motion around a preferred axial orientation such as it might occur in helices

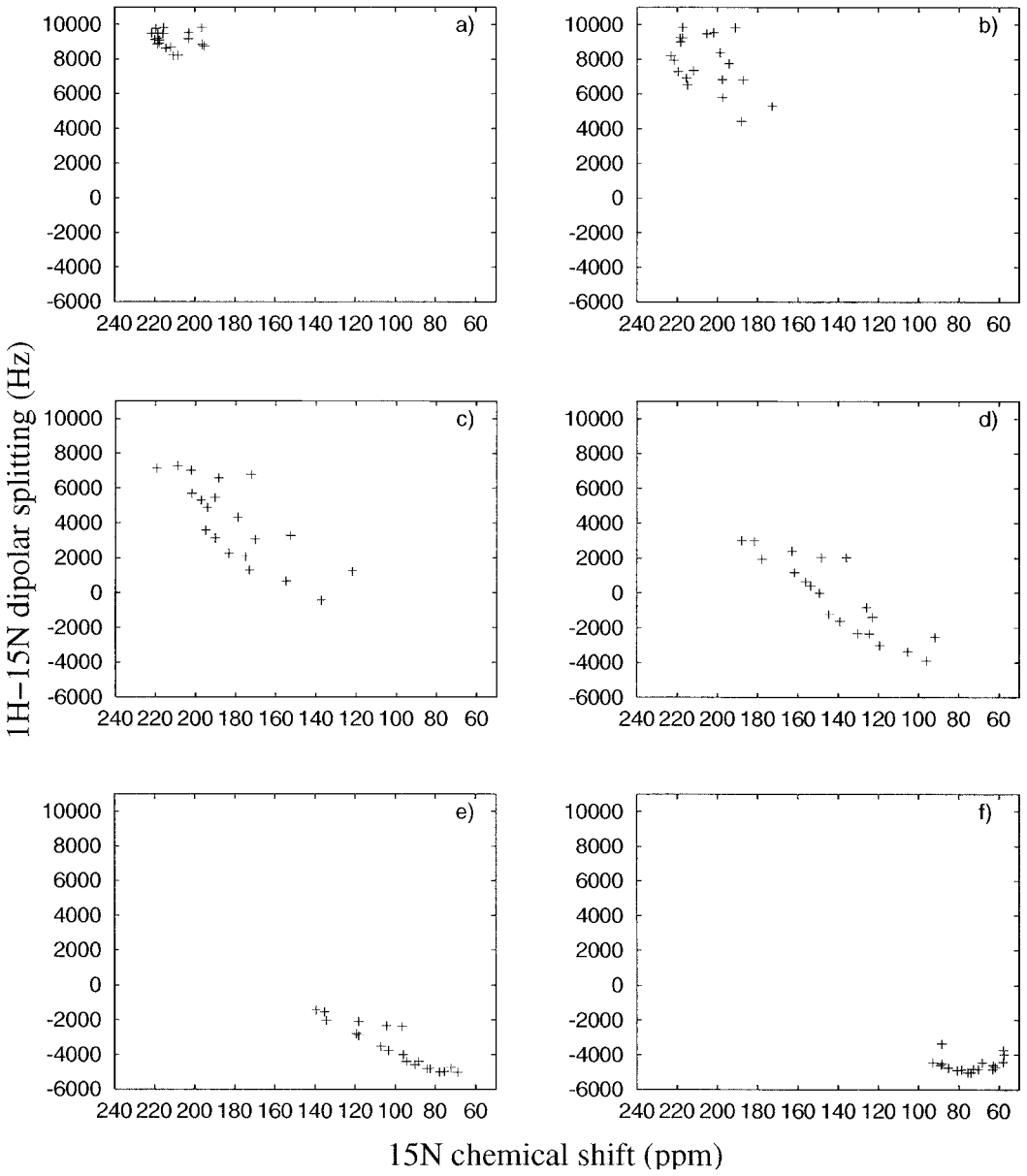

Figure 1. Simulated ^{15}N chemical shift/^{15}N-^{1}H dipolar spectra for helix D of bacteriorhodopsin (residues 106–126), in the static case (case 1 in Table 1). (a) $\xi = 0°$; (b) $\xi = 18°$; (c) $\xi = 36°$; (d) $\xi = 54°$; (e) $\xi = 72°$; (f) $\xi = 90°$.

forming a membrane pore. This type of motion (see supplemental material) has little effect on the positions of the CS/D pairs relative to the case of the static helix (case 1). In fact, the changes in the chemical shift values are of the order of 1–3 ppm and those for the dipolar splittings are less than or equal to 400 Hz, for a given value about a central value of ω ($\omega_0 = 0°$). If it is considered that typical experimental linewidths are of a similar order of magnitude, this would indicate that any axial motion around a fixed value of ω would not change the appearance of CS/D correlation spectrum relative to the static case. For completeness, the Gaussian distribution was replaced with a uniform distribution (centre value: 0°; width: $\pm 20°$). Similar results were obtained (data not shown).

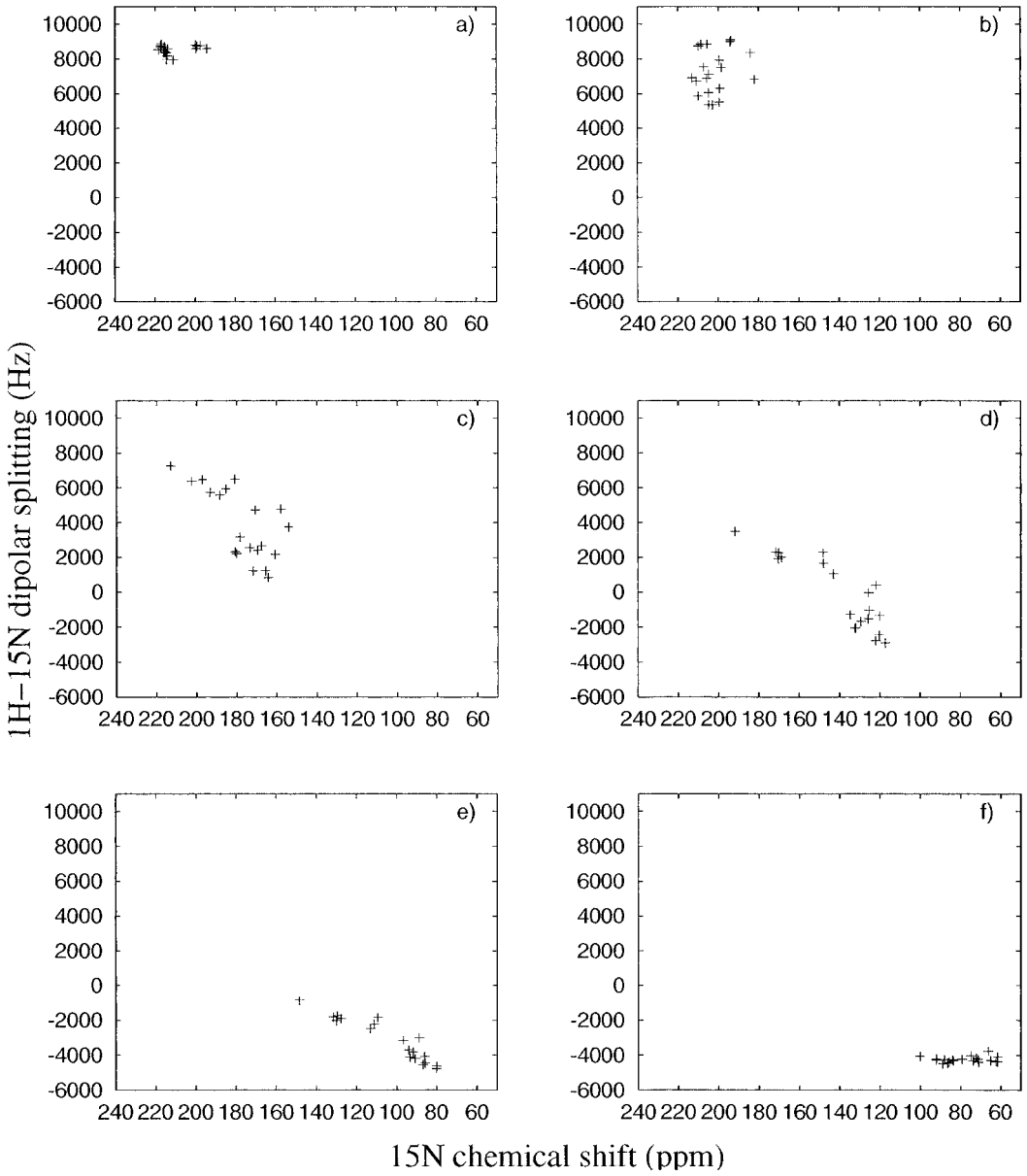

Figure 2. Simulated ^{15}N chemical shift/^{15}N-^{1}H dipolar spectra for helix D of bacteriorhodopsin (residues 106–126), in the case where librational motion of the peptide planes is considered (case 2 in Table 1). (a) $\xi = 0°$; (b) $\xi = 18°$; (c) $\xi = 36°$; (d) $\xi = 54°$; (e) $\xi = 72°$; (f) $\xi = 90°$.

Case 4: Fast tilt motion only

For motion about the angle ξ, two motional weighting schemes were considered. The first was a Gaussian distribution around ξ with widths of 10° (not shown) and 20° (see supplemental material). The second was a uniform distribution of width of 10° (not shown). This is used to simulate rapid Brownian motion about a preferred tilt angle ξ. In all cases, calculations were performed for central values of $\xi = 0°$–$90°$, in steps of 18°, with $\omega = 0°$.

A comparison of the spectra obtained in the static case and with these weighting schemes indicate that the measured NMR parameters are not very sensitive to rapid tilt motion. For the distributions about ξ considered here, the CS values change on the order of less than or equal to 1 ppm and the dipolar splittings shift

by 10–1000 Hz, with most shifts being on the order of 100–400 Hz. As a consequence, the patterns for the different ξ values are similar to those obtained for the static case.

Cases 5, 6, 7 and 8: Combinations of fast motions

Combinations of motions around ξ, ω, and π, summarised in Table 1, and their effect on the spectra were also simulated. Since the motions are assumed to be uncorrelated, the overall effect on the spectra is dominated by motion in the d.o.f. that produces the greatest shift of the CS/D pairs when considered alone. For example, a combination of all three fast motions resulted in spectra (see supplemental material) similar to those simulated for librational motion alone (Figure 2).

Comparison of the static and fast motional models

In order to characterise how the choice of motional model affects the value obtained for helix tilt ξ, the 'centres of mass' (c.o.m.) for all of the CS/D pairs were calculated for a given ξ. The 'centre of mass' was obtained by calculating the geometric mean of ν_i^{obs} for all of the planes of helix D in bR (residues 106–126). If the CS/D pairs would form a PISA wheel, then the corresponding c.o.m. would be the central point of the ellipse. In Figure 3, the c.o.m.'s for $\xi = 0°$–$90°$ for both case 1 (Figure 1) and case 8 are shown.

The models differ considerably for both small (0°–10°) and large (80°–90°) angles of tilt. Furthermore, the two c.o.m. lines diverge with increasing ξ. For example, the $\xi = 0°$ point obtained in the dynamic model corresponds to $\xi = 13°$ for the static model. Because of the divergence, a similar correspondence between the tilt angles predicted by the two models cannot be made for large angles. For mid-range values of ξ, the difference in tilt angle predicted is less pronounced. For instance, $\xi = 18°$ in the dynamic model corresponds to $\xi = 23°$ in the static model. The large difference of the models at the extremes of the range is of great practical importance, because most membrane protein helices lie roughly either perpendicular or parallel to the membrane normal. Thus, if an inappropriate model is chosen, the measurement of ξ will have large systematic errors associated with it in these cases.

Cases 9, 10, and 11: Spatial distributions

While librational motions are always likely to be present in biological systems, and to occur on a fast timescale, the other two degrees of freedom considered here may not occur on rapid timescales in membrane embedded proteins. Thus, spectra of spatial distributions (mosaic spread) in ξ and ω were simulated by plotting multiple points obtained from Equation 7 for discrete values of each angle respectively, as shown in Figures 4 and 5.

In the calculations performed here, the 'intensities' for each of the CS/D points in a line were assumed to be equal. Experimentally, the energetic difference between the conformations corresponding to these different ξ and ω angles means that the populations will vary (Straus et al., 1997). As a result, the experimental intensities will not be uniform and in the extreme case, only a single point might appear in the spectrum. These effects are ignored here; instead the lines drawn between data points indicate allowed regions for the spatial distributions chosen.

In Figure 4, a distribution in ξ was considered for central ξ values of 0° to 90°, incremented in steps of 18°. Points were calculated for each plane for the central ξ value ±10°, incremented in steps of 5°, and joined together in a line. The positions of the CS/D points are least sensitive to distributions in ξ for small central angles of ξ. Experimentally, this implies that slightly broader lines would be observed than in the case of fast motion at these angles (case 8). For larger values of ξ this line broadening effect would be more pronounced. Consequently, when determining the central value of ξ for small ξ these effects can be ignored. However, for larger central ξ values, line broadening effects make it difficult to determine the average tilt angle.

In Figure 5, a distribution in ω, centred around $\omega = 0° \pm 20°$, in steps of 5°, was considered. In this case, ξ was varied from 0°–90°, in steps of 18°, as in the previous sections. The points corresponding to the same plane were joined together in a line. Compared to spatial distributions in ξ, the two-dimensional map of CS/D points is less sensitive to changes in ω. For ξ close to 0° and 90°, the individual points are largely unaffected with respect to case 8 (no discernible line broadening). For intermediate values of ξ, the individual points migrate, but overall the points cover the same area. Consequently, distributions in ω can be ignored when determining helix tilt for all angles of ξ.

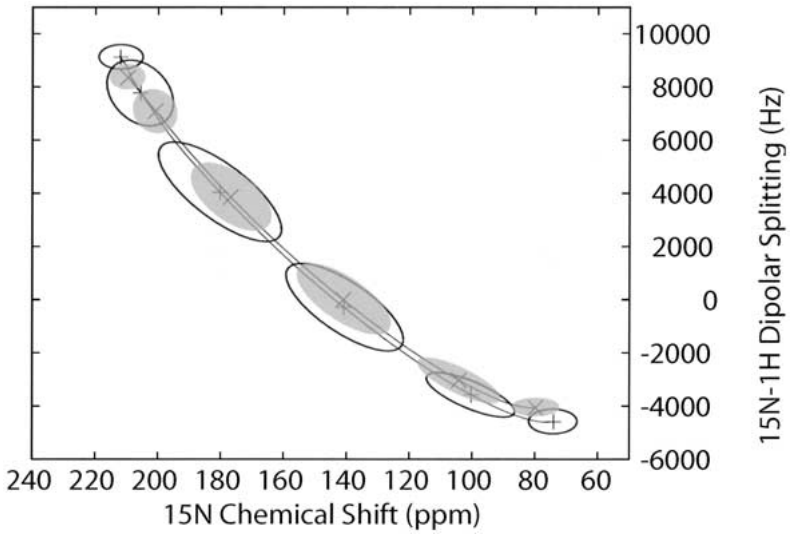

Figure 3. Comparison between the 'centre of mass' (c.o.m., see text) for the static case (+, open ellipses) and for the case where librational motion of the peptide planes, Gaussian motion around ω (width: 20°) and around ξ (width: 10°) are considered (x, filled ellipses). Data points were calculated from left to right for $\xi = 0°–90°$, in steps of 18°. The ellipses are centred on the c.o.m. and their extent is the minimum required to contain all calculated CS/D pairs of the helix at that angle. The models differ significantly for ξ close to 0° and close to 90°.

Discussion and conclusions

The effect of time and spatial averaging on the ^{15}N chemical shift and ^{15}N-^{1}H dipolar splitting for the chosen helix was found to be significant. The positions of the calculated CS/D pairs are heavily dependent on the chosen motional models. While experiment and MD agree on both the frequency and amplitude of the planar librational motions, experimental and theoretical information on the dynamics of axial rotation and helix tilt is scarce. A full investigation of these slower motions by computer simulation will necessitate a considerable increase in computer power. More extensive experimental studies on slow motional modes using relaxation measurements (Huster et al., 2001) may provide future insight. The differences between the Gaussian and uniform weighting schemes considered here were found to be small.

A number of checks were performed in order to test the system dependence of our results. Firstly, the effect of crystal structure resolution on the calculated NMR parameters for the static case was assessed. The same helix D was taken from three higher resolution structures (1C3W − resolution = 1.55 Å; 1F50 − resolution = 1.70 Å; 1QHJ − resolution = 1.90 Å). The extent of the patterns and the ordering of the CS/D pairs of these helices does not change significantly from one structure to the next (data not shown). Secondly, the divergence of the chosen helix from the ideal case was assessed. Two hundred and seventy (ϕ, ψ) pairs were taken from the helices in three atomic resolution crystal structures (1A6M, 1CEX and 1EXR, all at 1.0 Å resolution) and plotted with those of the chosen helix in a Ramachandran plot (see supplemental material). This shows that the spread of the (ϕ, ψ) pairs of the chosen helix is well within that of other experimentally determined helices. Finally, in order to assess whether the simulated librational motion is system dependent, a similar study was performed with another, smaller helix (taken from 1UD7) in water. The calculated NMR parameters, considering fast librational motion only, are qualitatively the same, with slightly larger averaging effects due to the higher mobility of the smaller helix. All of these checks suggest that the system bias is negligible in the results obtained here. We conclude that helix D from 1CWQ can be used as a model for a prototypical non-ideal helix undergoing various motional degrees of freedom.

Methanol was chosen as a solvent in this study for ease of computation. Previous computational studies have shown that the behaviour of membrane peptides does not significantly change when solvated in methanol or an explicit POPC bilayer (Biggin and Sansom, 1999). As a consequence, peptide simulations in more realistic lipid environments are not expected to yield significantly different results.

In this study, it was assumed that infinite dilution and uncorrelated motion of the helix holds for mem-

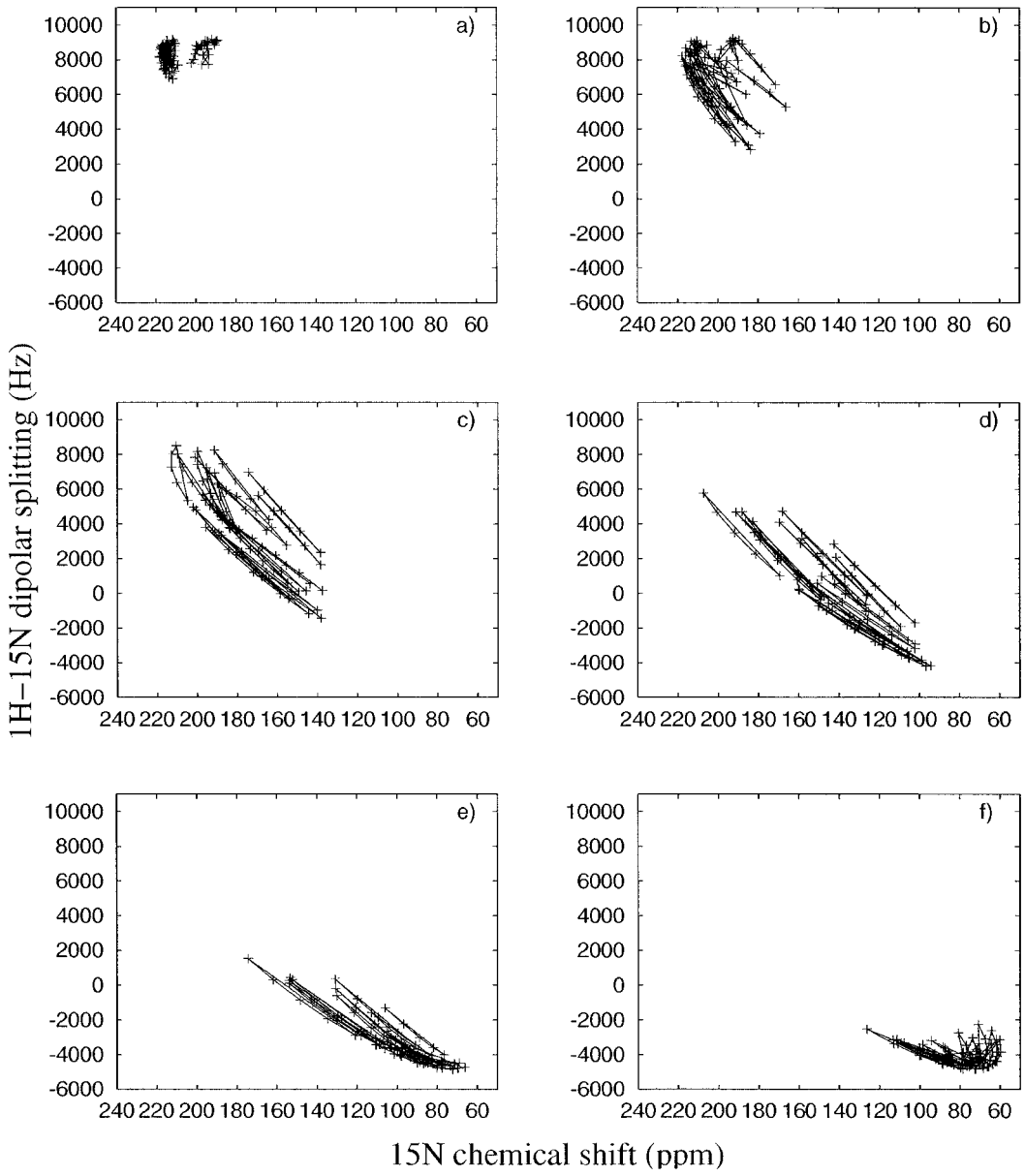

Figure 4. Simulated ^{15}N chemical shift/$^{15}N - {}^{1}H$ dipolar spectra for helix D ofbacteriorhodopsin (residues 106–126), in the case where a spatial distribution around ξ is considered (case 9 in Table 1). (a) $\xi = 0 \pm 10°$; (b) $\xi = 18 \pm 10°$; (c) $\xi = 36 \pm 10°$; (d) $\xi = 54 \pm 10°$; (e) $\xi = 72 \pm 10°$; (f) $\xi = 90 \pm 10°$.

brane embedded proteins. In practice, this condition is met where there is no aggregation of the peptides or proteins in the lipids, for example at lipid to peptide (protein) molar ratios greater than 200:1 (Lin and Baumgaertner, 2000). For samples with lower lipid to protein ratios, however, it is often not possible to conclusively test this assumption. Indeed, it could be argued that the high peptide content and low hydration conditions at which membrane protein samples are often prepared may encourage aggregation. This is most likely to have an effect on the axial rotation and helix tilt motions. As librational motion occurs even in densely packed crystals, this motional mode is still likely to be present at low lipid to protein ratios.

For the calculation of the CS/D pairs, it was also assumed that average CSA parameters and an average

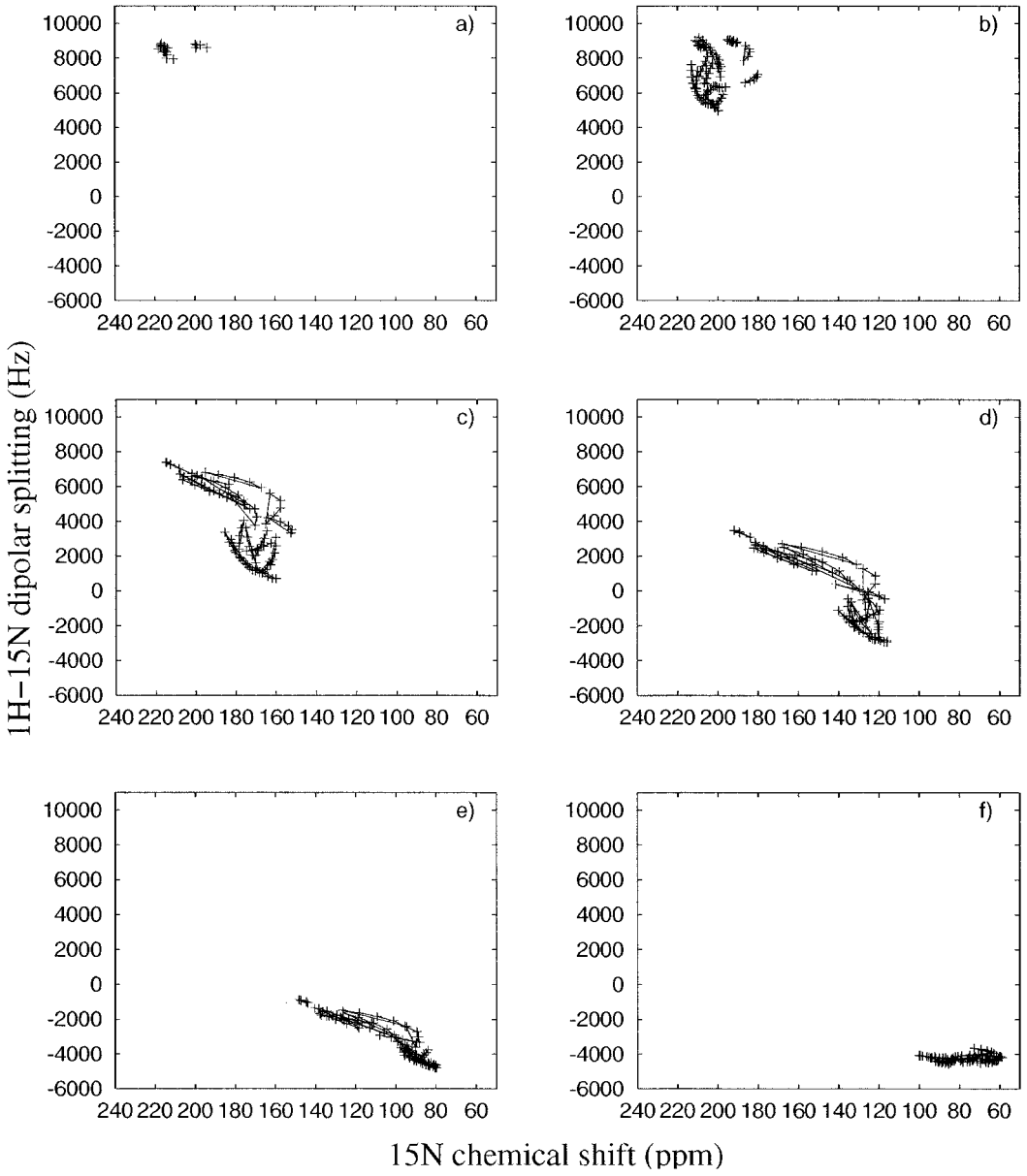

Figure 5. Simulated ^{15}N chemical shift/^{15}N-^{1}H dipolar spectra for helix D of bacteriorhodopsin (residues 106–126), in the case where a spatial distribution around $\omega = 0 \pm 20°$ is considered (case 10 in Table 1). (a) $\xi = 0°$; (b) $\xi = 18°$; (c) $\xi = 36°$; (d) $\xi = 54°$; (e) $\xi = 72°$; (f) $\xi = 90°$.

N-H bond length can be used. For the CSA parameters, this implies that σ_{11}, σ_{22}, σ_{33} and θ are independent of the amino acid residue type, with the exception of glycine which was treated separately, and of structural motif. By using an average value for the CSA parameters, system specific biases are reduced. In order to assess the influence of individual residue types on the calculated average, a series of tests were made. CSA values of one residue type, e.g., alanine, were removed from the complete set. The average CSA was calculated separately for both resulting subsets and used to calculate CS/D pairs over the valid range of (α,β). It was found that the difference in the calculated CS/D for alanine relative to all of the other amino acids was within the limit of what can currently be detected experimentally (i.e., for the CS, 1 ppm and for the D, 200 Hz). Similarly, the differences in CS/D for all (α,β) for the different structural motifs were

found to be small. More extensive CSA measurements in the future, either from solid or solution state NMR (Cornilescu and Bax, 2000, and references therein), or DFT calculations (Scheurer et al., 1999, and references therein; Brender et al., 2001) may allow the explicit consideration of the CSA parameters for each amino acid type and structural motif. At present, the use of average CSA parameters is sufficient. For the dipolar splitting calculation, the use of an average over a single value for the N-H bond length may be more questionable since the dipolar coupling is very sensitive to small changes in distance. Given the limited number of N-H bond lengths determined to date, however, it was felt that an average value would be more representative than a single one since system specific biases are removed. More extensive determinations of NH bond lengths by solid state NMR in the future will help to resolve this.

The results from the simulations performed here show that the ^{15}N chemical shift/^{15}N-^{1}H dipolar pairs are sensitive to the overall conformation of the helix and to time and spatial averaging effects. The largest effects observed were due to librational motion of the peptide planes. As the simulated r.m.s. librational amplitudes of between 10° and 14° are well within experimentally observed ranges, these averaging effects are also likely to be present on a similar order of magnitude in experimental data. On the other hand, localised motions around a fixed value of ω and ξ have little effect, indicating the chemical shift and dipolar splitting are insensitive to these types of motion. Overall, the simulations indicate that for a non-ideal helix, containing a number of glycine residues, the patterns formed by joining consecutive CS/D pairs do not form distinct PISA wheels. The unambiguous identification of all resonances on the basis of a single assignment is therefore difficult. In addition, the simulation results suggest that helix tilt can be determined from a comparison of experimental and simulated spectra without prior knowledge of assignments. The range, however, where clear distinctions can be made depends on the motional mode considered. Moreover, the angle determined for the helix tilt can be different by up to 10° depending on whether motion is considered in the model or not. Experimental data from solid state NMR as well as other methods could be useful to verify whether motion effects the helix tilt determination in this manner. For example, the difference reported in the helix tilt for Vpu determined from static PISA wheel simulations (tilt = 15°) (Marassi et al., 1999) and from site-directed Fourier transform infrared dichroism (tilt = 6.5° ± 1.7°) (Kukol and Arkin, 1999) might be accounted for by considering the effect of motion on NMR observables. A predicted helix tilt of 15° by the static model (case 1) corresponds most closely to a helix tilt of 7° when fast motion is considered (case 8) (Figure 3). Further simulations specific to Vpu could be undertaken to investigate this.

For an extensive structural study, a full spectral assignment and calculation of the three-dimensional structure are necessary. The approach outlined in (Marassi, 2001; Marassi and Opella, 2000; Wang et al., 2000) allows for a straightforward qualitative measure of membrane protein structure and topology. The model proposed here of a non-ideal helix undergoing librational motion, axial rotation and motion about the tilt angle offers an increased level of complexity. As more structural and dynamics studies of membrane peptides and proteins are undertaken, this model may prove useful in the comparison of experimental and simulated spectra in cases where motion cannot be neglected.

Acknowledgements

Very useful discussions with Burkhard Bechinger, James H. Davis and Wilfred F. van Gunsteren are gratefully acknowledged. The authors would also like to thank J.H. Davis and C. Fares for sharing recent work prior to publication. S.K.S gratefully acknowledges financial support from a Royal Society Dorothy Hodgkin Research Fellowship.

References

Bachar, M. and Becker, O.M. (2000) *Biophys. J.*, **78**, 1359–1375.
Bechinger, B. (2000) *Phys. Chem. Chemical Phys.*, **2**, 4563–4579.
Bechinger, B. and Sizun, C. (2002) *Concepts Magnetic Res.*, submitted.
Bielecki, A., Kolbert, A.C. and Levitt, M.H. (1989) *Chem. Phys. Lett.*, **155**, 341–346.
Biggin, P.C. and Sansom, M.S.P. (1999) *Biophys. Chem.*, **76**, 161–183.
Bowers, J.L. and Oldfield, E. (1988) *Biochemistry*, **27**, 5156–5161.
Brender, J.R., Taylor, D.M. and Ramamoorthy, A. (2001) *J. Am. Chem. Soc.*, **123**, 914–922.
Colnago, L.A., Valentine, K.G. and Opella, S.J. (1987) *Biochemistry*, **26**, 847–854.
Cordes, F.S., Kukol, A., Forrest, L.R., Arkin, I.T., Sansom, M.S.P. and Fischer, W.B. (2001) *Biochim. Biophys. Acta*, **1512**, 291–298.
Cornilescu, G. and Bax, A. (2000) *J. Am. Chem. Soc.*, **122**, 10143–10154.

Cross, T.A. and Opella, S.J. (1982) *J. Mol. Biol.*, **159**, 543–549.
Denny, J.K., Wang, J., Cross, T.A. and Quine, J.R. (2001) *J. Magn. Reson.*, **152**, 217–226.
Ernst, R.R., Bodenhausen, G. and Wokaun, A. (1987) *Principles of Nuclear Magnetic Resonance in One and Two Dimensions*, Oxford University Press, Oxford.
Glaubitz, C. and Watts, A. (1998) *J. Magn. Reson.*, **130**, 305–316.
Herzfeld, J., Mulliken, C.M., Siminovitch, D.J. and Griffin, R.G. (1987) *Biophys. J.*, **52**, 855–858.
Hubbell, W.L., Cafiso, D.S. and Altenbach, C. (2000) *Nat. Struct. Biol.*, **7**, 735–739.
Huster, D., Xiao, L. and Hong, M. (2001) *Biochemistry*, **40**, 7662–7674.
Ishii, Y., Terao, T. and Hayashi, S. (1997) *J. Chem. Phys.*, **107**, 2760–2774.
Johnson Jr, J.P. and Zagotta, W.N. (2001) *Nature*, **412**, 917–21.
Jones, D.H., Barber, K.R., VanDerLoo, E.W. and Grant, C.W. (1998) *Biochemistry*, **37**, 16780–16787.
Kukol, A. and Arkin, I.T. (1999) *Biophys. J.*, **77**, 1594–1601.
Kumashiro, K.K., Schmidt-Rohr, K., Murphy III, O.J., Ouellette, K.L., Cramer, W.A. and Thompson, L.K. (1998) *J. Am. Chem. Soc.*, **120**, 5043–5051.
Lin, J.H. and Baumgaertner, A. (2000) *Biophys. J.*, **78**, 1714–1724.
Litman, B.J. and Mitchell, D.C. (1996) *Lipids*, **31**, S193–197.
Marassi, F.M. (2001) *Biophys. J.*, **80**, 994–1003.
Marassi, F.M. and Opella, S.J. (2000) *J. Magn. Reson.*, **144**, 150–155.
Marassi, F.M., Ma, C., Gratkowski, H., Straus, S.K., Strebel, K., Oblatt-Montal, M., Montal, M. and Opella, S.J. (1999) *Proc. Natl. Acad. Sci. USA*, **96**, 14336–14341.
Marsh, D. (1990) *CRC Handbook of Lipid Bilayers*, CRC Press Ltd., London.
North, C.L. and Cross, T.A. (1995) *Biochemistry*, **34**, 5883–5895.
Opella, S.J., Marassi, F.M., Gesell, J.J., Valente, A.P., Kim, Y., Oblatt-Montal, M. and Montal, M. (1999) *Nat. Struct. Biol.*, **6**, 374–379.
Prosser, R.S. and Davis, J.H. (1994) *Biophys. J.*, **66**, 1429–1440.
Prosser, R.S., Davis, J.H., Dahlquist, F.W. and Lindorfer, M.A. (1991) *Biochemistry*, **30**, 4687–4696.
Qui, X.Q., Jakes, K.S., Kienker, P.K., Finkelstein, A. and Slatin, S.L. (1996) *J. Gen. Phys.*, **107**, 318–328.
Ramamoorthy, A., Gierasch, L.M. and Opella, S.J. (1996) *J. Magn. Reson.*, **B111**, 81–84.
Ramamoorthy, A., Wu, C.H. and Opella, S.J. (1999) *J. Magn. Reson.*, **140**, 131–140.
Saito, H., Tuzi, S., Yamaguchi, S., Tanio, M. and Naito, A. (2000) *Biochim. Biophys. Acta*, **1460**, 39–48.
Sass, H.J., Buldt, G., Gessenich, R., Hehn, D., Neff, D., Schlesinger, R., Berendzen, J. and Ormos, P. (2000) *Nature*, **406**, 649–653.
Scheurer, C., Skrynnikov, N.R., Lienin, S.F., Straus, S.K., Brüschweiler, R. and Ernst, R.R. (1999) *J. Am. Chem. Soc.*, **121**, 4242–4251.
Schiffer, M. and Edmundson, A.B. (1967) *Biophys. J.*, **7**, 121–135.
Scott, W.R.P., Hünenberger, P.H., Tironi, I.G., Mark, A.E., Billeter, S.R., Fennen, J., Torda, A.E., Huber, T., Krüger, P. and van Gunsteren, W.F. (1999) *J. Phys. Chem.*, **A103**, 3596–3607.
Shen, L.Y., Bassolino, D. and Stouch, T. (1997) *Biophys. J.*, **73**, 3–20.
Sizun, C. and Bechinger, B. (2002) *J. Am. Chem. Soc.*, **124**, 1146–1147.
Smith, R., Separovic, F., Milne, T.J., Whittaker, A., Bennett, F.M., Cornell, B.A. and Makriyannis, A. (1994) *J. Mol. Biol.*, **241**, 456–466.
Song, Z.Y., Kovacs, F.A., Wang, J., Denny, J.K., Shekar, S.C., Quine, J.R. and Cross, T.A. (2000) *Biophys. J.*, **79**, 767–775.
Straus, S.K., Bremi, T. and Ernst, R.R. (1997) *J. Biomol. NMR*, **10**, 119–128.
Tieleman, D.P., Shrivastava, I.H., Ulmschneider, M.R. and Sansom, M.S.P. (2001) *Proteins*, **44**, 63–72.
van Gunsteren, W.F., Billeter, S.R., Eising, A.A., Hünenberger, P.H., Krüger, P., Mark, A.E., Scott, W.R.P. and Tironi, I.G. (1996) *Biomolecular Simulation: The GROMOS96 Manual and User Guide*, VdF: Hochschulverlag AG an der ETH Zürich and BIOMOS b.v, Zürich, Groningen.
Wang, J., Denny, J., Tian, C., Kim, S., Mo, Y., Kovacs, F., Song, Z., Nishimura, K., Gan, Z., Fu, R., Quine, J.R. and Cross, T.A. (2000), *J. Magn. Reson.*, **144**, 162–167.
Watts, A. (1998) *Biochem. Biophys. Acta*, **1376**, 297–318.
Waugh, J.S. (1976) *Proc. Natl. Acad. Sci. USA*, **73**, 1394–1397.
Woolf, T.B. and Roux, B. (1994) *Proc. Natl. Acad. Sci. USA*, **91**, 11631–11635.